Available online at www.sciencedirect.com
SCIENCE DIRECT®
Pergamon
Cement and Concrete Research 33 (2003) 1127–1136
CEMENT AND CONCRETE RESEARCH

Volume and deviator creep of calcium-leached cement-based materials

Olivier Bernard, Franz-Josef Ulm*, John T. Germaine

Massachusetts Institute of Technology, Cambridge, MA 02139, USA

Received 8 May 2002; accepted 7 January 2003

Abstract

This paper provides new experimental evidence of the specific volume creep and deviator creep of cement-based materials. Creep tests conducted on calcium-leached cement pastes and mortars under various triaxial loading conditions provide conclusive evidence of a specific short-term creep and a specific long-term creep. It is found that at least two competing dissipative mechanisms are at work in short-term creep of cement-based materials: (1) a creep relaxation mechanism in the calcium–silicate–hydrate (C–S–H) solid phase activated by microstress concentrations in the heterogeneous microstructure; and (2) stress relaxation by microcracking beyond a relatively small stress threshold. If the first dominates over the second, the short-term volume creep is contracting, and in the inverse case, a short-term dilating behavior is found. Furthermore, provided that microcracking stabilizes during the short-term creep, the long-term creep occurs at constant volume. Based on these results, we argue that the concept of a creep Poisson's ratio, which is commonly employed in engineering practice to extrapolate uniaxial creep tests to multiaxial stress conditions, should be abandoned when triaxial stress states affect the durability performance of concrete structures.

Keywords: Creep; Cement paste; Mortar; Microcracking; Interfacial transition zone; Triaxial testing

1. Introduction

The basic creep of concrete, which is the time-dependent deformation of a sealed concrete specimen under constant applied load, is classically investigated by a normalized creep test, in which the strain in the uniaxial compression in the direction of load application is recorded (see, for instance, Ref. [1]). For engineering design purposes, the uniaxial stress–strain response is extrapolated to three dimensions, by analogy with linear isotropic elasticity, by means of a creep Poisson's ratio (CPR; see, for instance, Ref. [2]), which in a uniaxial test represents the ratio of transversal to axial strains. The CPR has been used in many applications, such as biaxially prestressed nuclear containment structures [3] and repaired concrete elements [4], in which triaxial stresses are critical for the determination of the long-term deformation behavior of concrete and the durability performance of concrete structures.

The very use of the CPR is based on the assumption of the stress linearity of creep. And from a creep kinetics standpoint, it implies that the physical mechanisms at the origin of basic creep are the same irrespective of the direction of load application (isotropic creep behavior), and for both the volume and deviator part of creep. Considerable experimental research has been devoted to the determination of the CPR in the late 1960s and 1970s (for a review of existing data, see Ref. [5]). The large scattering of experimental results, $\nu_c \in [0,0.36]$, highlights the difficulty of accurately measuring transversal strains in uniaxial creep tests. This scattering, however, may also be associated with a limit of relevance of the CPR with regard to the physical mechanisms causing creep. For instance, Gopalakrishnan et al. [6] and Chuang et al. [7] showed that creep under multiaxial compression is less than creep in uniaxial compression of the same magnitude in a given direction. The authors conclude that the CPR was a function of stress, thus questioning the linearity of creep under multiaxial stress conditions. This conclusion, however, appears to be related to the very use of the CPR to capture multiaxial creep, rather than conclusive evidence of the nonlinearity of creep with regard to stress.

The multiaxial creep deformation behavior in uniaxial compression was studied, beyond the concept of CPR, by Ulm et al. [8,9] on ordinary concrete. Measurements of the

* Corresponding author. Tel.: +1-617-253-3544; fax: +1-617-253-6044.
E-mail address: ulm@mit.edu (F.-J. Ulm).
URL: http://cist.mit.edu.

0008-8846/03/$ – see front matter © 2003 Elsevier Science Ltd. All rights reserved.
doi:10.1016/S0008-8846(03)00021-8

axial and radial strains showed that the short-term creep of concrete was characterized by a dilatant behavior (i.e., a positive volume increase rate over about 1 week), while the long-term creep was found to occur at constant volume. Rossi and Acker [10] reported a correlation over a 2-week period of measurements between the succession of cracking events and the evolution of axial strains in uniaxial compression creep. The short-term creep associated with a dilating behavior, therefore, may well be due to microcracking. On the other hand, the constant volume of long-term creep suggests a pure viscous shear mechanism acting in the space of the calcium–silicate–hydrate (C–S–H) [2]. The experimental evidence to support these suggestions, however, is based on a short period of measurements and restricted to uniaxial compression creep of unleached concrete.

The objective of this paper is to provide new evidence of the specific volume and deviator creep from multiaxial tests, and to relate the specific behavior to the rate determining physical processes that cause creep. To this end, drained creep tests under sustained triaxial stress states are conducted on calcium-leached cement paste and mortar. The employed leaching process dissolves the Portlandite crystals $Ca(OH)_2$ and decalcifies the C–S–H of the cement paste. The rationale behind the employment of calcium-leached materials is that C–S–H, in unleached materials, is known to be the only component of cement-based materials that exhibits creep [11], and that the rather large and stiff Portlandite crystals $Ca(OH)_2$ reduce the creep magnitude along grain boundaries, similar to the role of rigid inclusions in a matrix. Leaching, therefore, is expected to magnify the triaxial creep response while preserving the relevant deformation characteristics of creep of nondegraded cement-based materials. In addition, the creep results of leached materials may also be used for the prediction of the long-term behavior of aging materials in concrete structures, relevant, for example, in monitoring the durability performance of nuclear waste containment structures [12].

The paper is organized as follows. In Section 2, the composition of the materials is presented, together with the employed triaxial creep test device. The results of the series of tests of hydrostatic creep and deviator compression creep are analyzed in Section 3. The discussion in Section 4 links the observed creep behavior to the creep mechanisms. Finally, several relevant conclusions are drawn for the transposition of the results obtained on calcium-leached specimens to nondegraded materials.

2. Materials and test procedure

2.1. Materials and specimen preparation

Cement paste and mortar were prepared at a water–cement ratio w/c = 0.5, using an ordinary Type I Portland cement. The composition of the cement is given in Table 1. The mortar composition is characterized by a water–cement–sand mass ratio of w/c/s = 1/2/4, using a fine Nevada sand of density 2650 kg/m^3, $d_{60} = 0.23$ mm, and $d_{30} = 0.17$ mm. This corresponds roughly to a (sand) inclusion fraction of $f_I \simeq 0.5$. The specimens were cast in cylindrical molds of 11.5 mm diameter and 60 mm length. After 24 h, the specimens were removed from the mold and cured in lime water for 28 days. After curing, the specimens were placed in 6 M ammonium nitrate solution for calcium leaching. In this accelerated leaching test, described in detail in Ref. [13], 'natural' leaching by pure water is accelerated by a factor of 300, with a Portlandite dissolution front that reaches the center of the 11.5-mm-diameter samples after 9 days. The partial dissolution of the calcium in the C–S–H requires 45 days, resulting in complete and uniform calcium-leached samples.

Table 1
Type I Portland cement constituents, in mass percent (data provided by cement producer)

OPC Type I					
CaO	SiO_2	Al_2O_3	MgO	SO_3	Na_2O
62.3	20.8	4.4	3.8	2.9	0.39
Fe_2O_3	K_2O	C_3Al	C_3S	C_2S	Ignition loss
2.4	1.28	8	53	20	0.66

The triaxial strength properties of calcium-leached cement paste and mortar materials were reported in Refs. [12,14], in the form of the Drucker–Prager strength parameters, cohesion c and friction coefficient δ:

$$f = \sqrt{J_2} + \delta\sigma'_m - c = 0 \quad (1)$$

where $J_2 = (1/2)s_{ij}s_{ij}$ is the stress deviator invariant, and $\sigma'_m = (1/3)\sigma_{kk} + p$ is the effective mean stress ($s_{ij} = \sigma_{ij} - \sigma'_m\delta_{ij}$ = stress deviator; p = interstitial fluid pressure; δ_{ij} = Kronecker delta). These strength parameters, which will be used to define the deviator stress-to-strength ratio, are summarized in Table 2, together with the uniaxial compressive strength f_c and the initial porosity ϕ_0.

After 45 days of accelerated leaching, the samples were kept in the ammonium nitrate solution until the beginning of the creep test. The age of the samples at this time was at least 73 days. Given the leached material state, it is reasonable to consider the difference of age at the time of loading and autogeneous shrinkage during the test insignificant. In addition, drying was prevented by ensuring saturated conditions before and during the test. Prior to testing, the samples were cut with a diamond saw to a size of 11.5 × 23.5 mm, to obtain smooth surfaces and parallel ends.

2.2. Triaxial creep test device

The triaxial creep test device, shown in Fig. 1, is adopted from the experimental setup of Heukamp et al. [13]

Table 2
Compressive strength f_c, cohesion c, friction coefficient δ, and initial porosity ϕ_0 (accessible to water) of unleached and leached materials

		f_c [MPa]	c [MPa]	δ [1]	ϕ_0 [%]
Cement paste	Unleached	54.1	17.1	0.82	38.9
	Leached	3.3	1.1	0.56	63.3
Mortar	Unleached	36.6	9.8	1.10	27.6
	Leached	3.4	0.96	0.81	39.5

developed for the assessment of the triaxial strength domain of calcium-leached cement-based materials. The triaxial cell is equipped with an internal load cell, a chamber pressure transducer, and a pore pressure transducer. In addition, the axial (i.e., vertical) displacement is measured at the cross-head with an LVDT. The saturated material specimen, a porous stone, and steel caps are placed in a latex membrane (see Fig. 1). The steel cap under the porous stone contains a hole, which allows water transport to and from the specimen. This allows monitoring of the interstitial fluid pressure and the change in water content of the specimen, and gives access to the relative volume variation. The sample is placed in the triaxial cell, and the steel chamber is filled with silicon oil. A low hydrostatic pressure ($\sigma_m = -0.5$ MPa), which is equilibrated by a pore pressure of the same magnitude ($p = 0.5$ MPa) so that the effective mean stress ($\sigma'_m = \sigma_m + p$) is zero, is applied for 24 h, establishing a reference state in terms of water content m_{f0}, (Lagrangian) porosity ϕ_0, and initial strain ε^0_{ij}.

The triaxial load application is not instantaneous and comprises two phases. First, a hydrostatic stress is applied at a loading rate of 5 kPa/s by increasing the oil pressure to the target level of the radial confinement $\bar{\sigma}_{rr}$ in the specific test. During this loading phase, the pore pressure p is kept constant. Then, while keeping both the confinement $\bar{\sigma}_{rr}$ and the pore pressure p constant, an additional axial load, if any, is applied until the target level of the deviator stress $\Delta\sigma = \bar{\sigma}_{zz} - \bar{\sigma}_{rr}$ is reached. The deviator stress $\Delta\sigma$ is applied displacement driven at a constant strain rate of 5×10^{-6} s^{-1}. The loading takes roughly 5–10 min for each test to reach the target value after which the applied stress remains constant. A consolidation time of 2–3 h is required to reestablish drained conditions from any potential excess pore pressure introduced during loading [13]. The deformation that occurs during this consolidation phase will not be considered in the creep analysis, as it relates rather to the loading conditions and the resulting elastic deformation, than to the intrinsic creep behavior of the tested materials.

The stress level defined by the effective mean stress $\sigma'_m = \sigma_{rr} + p + (1/3)\Delta\sigma$ and the deviator stress $\Delta\sigma$ is kept constant in the creep test through a computer-controlled algorithm. In particular, the displacement-controlled axial deformation is continuously adjusted to keep constant the axial stress level $\bar{\sigma}_{zz} = \bar{\sigma}_{rr} + \Delta\sigma$. Initialized at the end of loading, the measurement device gives direct access to the vertical strain variation $\delta\varepsilon_{zz} = \varepsilon_{zz} - \varepsilon^0_{zz}$. We will refer to $\delta\varepsilon_{zz}$ as axial creep strain in what follows. The second deformation quantity that is continuously recorded is the change in Lagrangian porosity, which is accessible by monitoring the water content m_f of the sample under drained conditions, p = constant, from (see, e.g., Ref. [15]):

$$\delta\phi = \phi - \phi_0 = \frac{m_f - m_{f0}}{\rho_{fl}(p_0)} \tag{2}$$

where $\rho_{fl}(p_0)$ is the water mass density, which depends on the fluid pressure p_0. It is worthwhile to note that the change in Lagrangian porosity refers to the current volume oc-

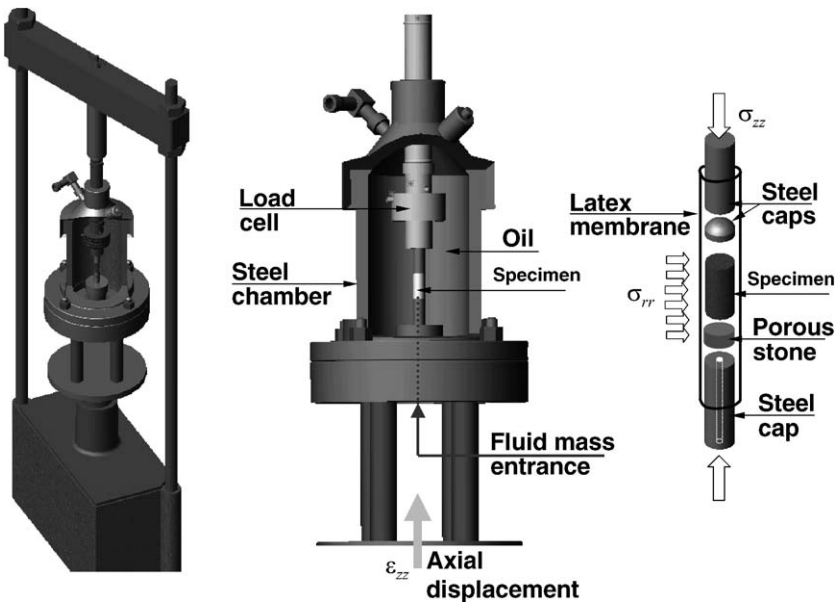

Fig. 1. Experimental setup [13] employed for triaxial creep tests.

cupied by the fluid phase at time t normalized by the initial volume V_0; or, equivalently, expressed in terms of the total volume strain $\varepsilon = \varepsilon_{kk}$ of the sample, and the solid deformation:

$$\delta\phi = \delta\varepsilon - \frac{\delta V_s}{V_0} \tag{3}$$

where $\delta V_s = V_s - V_{s0}$ is the change in volume occupied by the solid phase in the material sample. For an incompressible solid phase $\delta V_s = 0$, which has been found to hold for calcium-leached cement paste and mortars [13]. In this case, the change in porosity $\delta\phi$ coincides with the relative volume change $\delta\varepsilon = \varepsilon - \varepsilon^0$, and will serve as background for the analysis of the triaxial creep test results.

The test duration was roughly 30 days, and the tests were carried out in an environmentally controlled chamber at constant temperature of 22 ± 1 °C. Repeatability of the testing procedure was checked by running similar creep tests in different load frames.

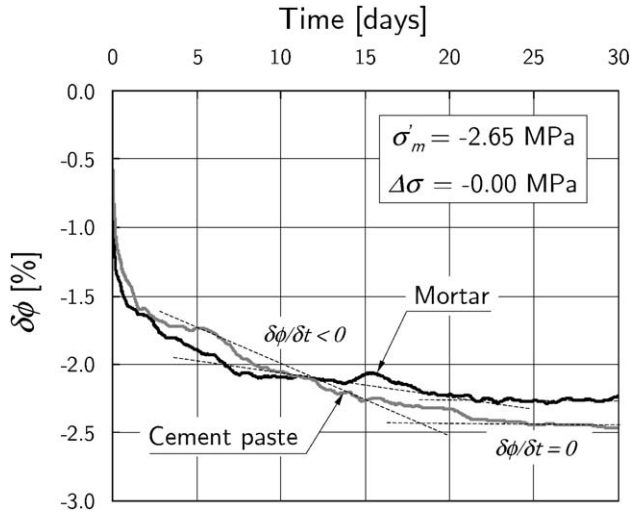

Fig. 2. Change in porosity during hydrostatic creep tests of cement paste and mortar.

3. Results

3.1. Contraction in hydrostatic compression creep

Leached cement-based materials in hydrostatic compression exhibit a short-term contracting behavior, which stops after some 23 days.

Hydrostatic creep tests were conducted on cement paste and mortar at a low level of effective mean stress $\sigma'_m = -2.65$ MPa and $\Delta\sigma = 0$. This mean stress level is on the order of the elastic limit of calcium-leached cement pastes in hydrostatic compression and induces a permanent contraction of the cement paste that densifies in mortar the interfacial transition zone (ITZ) between sand grains and cement paste matrix [14]. The change of porosity $\delta\phi$ recorded in the creep tests on both materials is displayed in Fig. 2. We note:

1. Following a relatively steep change of porosity during the first 2 h, which can be attributed to water movement due to consolidation, mortar contracts more than cement paste in the first 10 days. This observation is at first surprising, given the reinforcing effect of (almost) rigid sand particles in a soft calcium-leached cement paste matrix. The observation is, however, consistent with the role of the ITZ on the deformation behavior of mortars. The ITZ is the weakest and the most porous zone of the composite material [16] and its properties govern the very short-term volume creep response of mortar.
2. Between 5 and 21 days, the contraction rate $\delta\phi/\delta t < 0$ is higher in the cement paste than in the mortar. The short-term contracting creep in hydrostatic compression, therefore, results from creep of the cement paste matrix, and is scaled by the matrix volume fraction.
3. After 23 days, the change of porosity almost stops ($\delta\phi/\delta t \to 0$), indicating an end of volume creep.

In summary, given the macroscopic hydrostatic stress, it seems that leached cement-based materials have only a short-term contracting creep.

3.2. Dilatation in deviator compression creep

Leached mortar, in contrast to cement paste, exhibits a short-term dilating behavior in triaxial compression. Long-term creep of both materials occurs at constant volume, indicating a pure deviator creep mechanism at work.

Deviator compression creep tests were conducted on cement paste and mortar at the same level of effective mean stress $\sigma'_m = -2.65$ MPa as in the hydrostatic test. In addition, a deviator stress of $\Delta\sigma = -2.0$ MPa is applied. The deviator stress-to-strength ratio n is evaluated from the distance to the loading surface (Eq. (1)), noting that in the triaxial test $\sqrt{J_2} = \sqrt{\frac{1}{3}}|\Delta\sigma|$:

$$n = \frac{|\Delta\sigma|}{\sqrt{3}(c - \delta\sigma'_m)} \tag{4}$$

With the values of Table 2, the deviator stress level corresponds to, respectively, $n = 45\%$ and $n = 37\%$ of the deviator strength of the cement paste and the mortar.

The change of porosity $\delta\phi$ and the evolution of axial creep strain $\delta\varepsilon_{zz}$ are shown in Figs. 3 and 4, respectively. After the initial consolidation contraction, there is a significant difference in the response of cement paste and mortar:

1. For cement paste, the volume creep in Fig. 3 shows strong similarities with the hydrostatic creep response (see Fig. 2), that is, an overall contracting behavior $\delta\phi/\delta t < 0$ during 21 days, followed by no significant change of porosity afterwards ($\delta\phi/\delta t = 0$). In contrast to hydrostatic creep, however, the axial creep $\delta\varepsilon_{zz}$ continues even

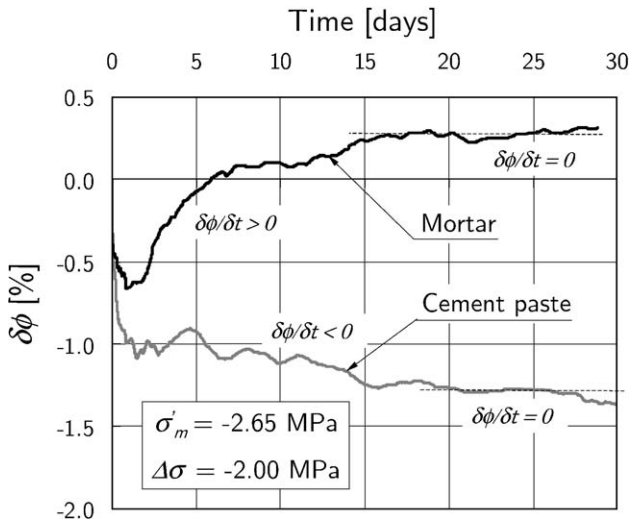

Fig. 3. Change of porosity during deviator creep tests of cement paste and mortar.

after 21 days (see Fig. 4). The cement paste creep response, therefore, is characterized by two phases—a short-term volume creep contraction, followed by creep at constant volume, which may be suitably called deviator creep.

2. The creep response of the mortar is quite different. In contrast to the cement paste, the mortar exhibits a short-term dilating behavior (i.e., $\delta\phi/\delta t>0$) during the same time, 21 days. After this short-term dilating creep, the volume stabilizes (i.e., $\delta\phi/\delta t=0$). The axial creep $\delta\varepsilon_{zz}$ of the mortar is smaller than the one of the cement paste (see Fig. 4), but continues also after 21 days at constant volume.

The short-term dilating creep behavior of mortar confirms results by Ulm et al. [8], which were obtained by another measurement device (axial and transversal strain measurements) for another cement-based material (ordinary concrete) subjected to other loading conditions (uniaxial compressive stress). We find the same behavior for calcium-leached mortars in triaxial compression, but not for cement paste. It is therefore likely that the short-term creep dilatation is related to the presence of inclusions (sand particles, aggregates) in cement-based composites, or, more precisely, to the presence of an ITZ surrounding the inclusions.

On the other hand, the long-term creep behavior of both cement paste and mortar occurs at constant volume. This purely deviator creep has also been found for concrete [8].

3.2.1. Threshold of short-term creep dilatation

Application of a stress deviator leads to a reduction of the contracting behavior, and a threshold exists beyond which the overall volume creep response of mortars becomes dilatant.

A refined analysis of the volume creep behavior of cement paste and mortar is obtained from a comparison of the porosity change between the hydrostatic and the deviator compression creep tests, shown in Figs. 5 and 6. For purpose of comparison, the porosity change of the hydrostatic test is initialized at the same radial confinement pressure $\sigma_{rr}=\sigma'_m-(1/3)\Delta\sigma=-1.98$ MPa, which corresponds to the onset of deviator stress application $\Delta\sigma$. Fig. 6 also displays the porosity change for a lower deviator stress level $\Delta\sigma=-0.50$ MPa but the same mean stress $\sigma'_m=-2.65$ MPa, which corresponds to a deviator stress-to-strength ratio of $n=9.3$ (compared to $n=37\%$).

We first note that the volume creep under deviator loading is generally smaller than in hydrostatic compression, which indicates that its magnitude depends on the deviator stress level. This deviator stress level affects the

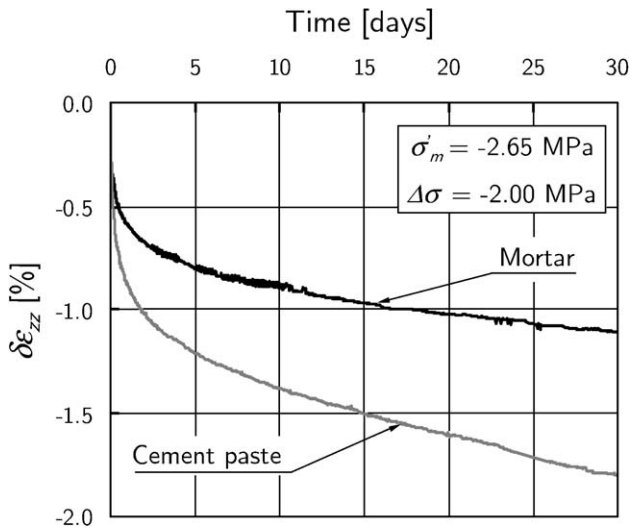

Fig. 4. Evolution of axial strain during deviator creep tests of cement paste and mortar.

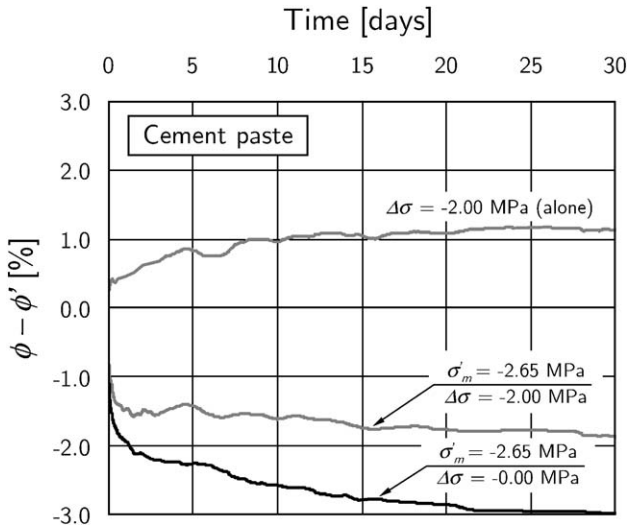

Fig. 5. Change of porosity during volumetric and deviator creep tests of cement paste.

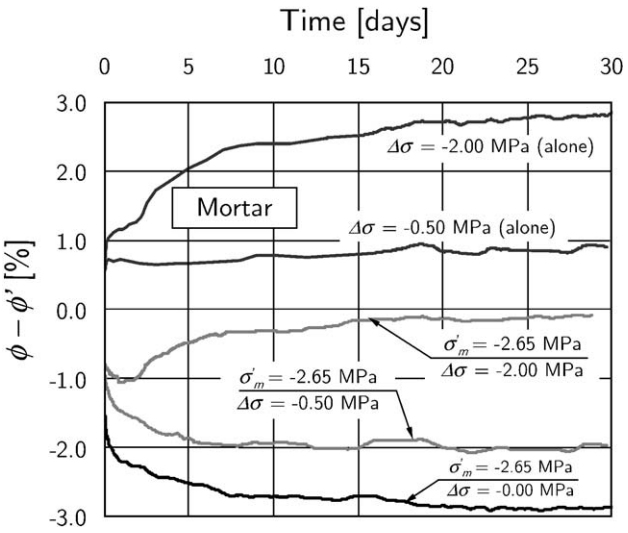

Fig. 6. Change of porosity during volumetric and deviator creep tests of mortar.

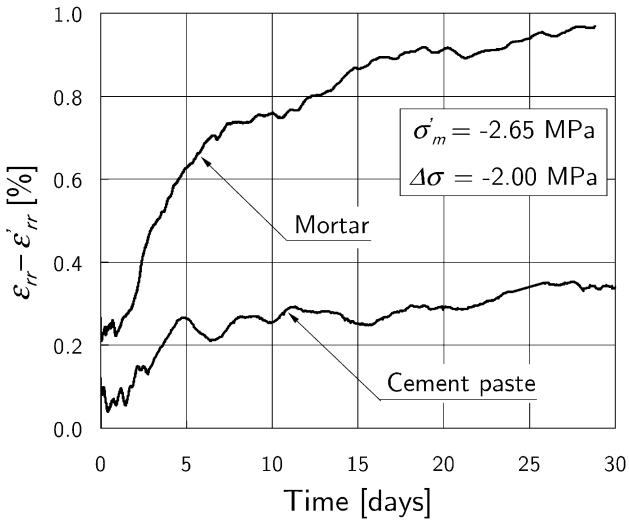

Fig. 7. Radial creep of cement paste and mortar.

short-term creep response: at low deviator stress-to-strength ratio ($n = 9.3\%$), mortar exhibits a pure contracting behavior, similar to the hydrostatic response $n = 0\%$; and for a higher deviator stress-to-strength ratio of $n = 37\%$, the mortar develops an overall short-term dilating behavior (see Fig. 6). The switch from a contracting behavior (induced by hydrostatic confinement) to a dilating behavior indicates the existence of a deviator stress (or shear stress) threshold for mortar.

To amplify the effect of $\Delta\sigma$ on the volume change, Figs. 5 and 6 also display the deviator stress-induced change in porosity, obtained by subtracting from the porosity change response in deviator compression the porosity change in hydrostatic compression. The result indicates an overall dilating behavior induced by deviator stress application, and this is for both cement paste and mortar.

3.2.2. Stress-induced anisotropy of deviator compression creep

In contrast to the axial contraction, the radial creep expansion of mortar is greater than the one of cement paste, which indicates a stress-induced anisotropic creep behavior in triaxial compression.

Fig. 7 compares the radial creep of cement paste and mortar, calculated from the measured axial creep strain $\delta\varepsilon_{zz}$ and the porosity change $\delta\phi(t) \approx \delta\varepsilon$ (see Eq. (3)):

$$\delta\varepsilon_{rr}(t) = \frac{1}{2}\left(\delta\phi(t) - \delta\varepsilon_{zz}(t)\right) \tag{5}$$

The radial strain evolution needs to be compared with the axial strain evolution displayed in Fig. 4. While the axial contraction is greater in the cement paste than in the mortar, the radial expansion $\delta\varepsilon_{rr}(t)$ is greater in the mortar. In terms of ratio between radial and axial short-term creep strain (see Fig. 8), the result would correspond to $\delta\varepsilon_{rr}(t)/\delta\varepsilon_{zz}(t) \simeq -0.25$ for the cement paste, and $\delta\varepsilon_{rr}(t)/\delta\varepsilon_{zz}(t) \simeq -2.00$ for the mortar. The high value for mortar can be attributed to the permanent dilating behavior induced by deviator stress application, which results in a stress-induced anisotropic creep behavior of cement-based composites.

3.3. Influence of the confinement pressure on the dilating behavior

The ITZ has been found to play a critical role in the short-term creep behavior of calcium-leached mortar. The investigation of the ITZ presented below consists of studying the following two limit cases: (1) the case of a mortar in which the ITZ has been precompacted, and thus mechanically deactivated; and (2) the case of a mortar and cement paste, in which the confinement pressure is reduced to a level that the dilating behavior can lead to failure.

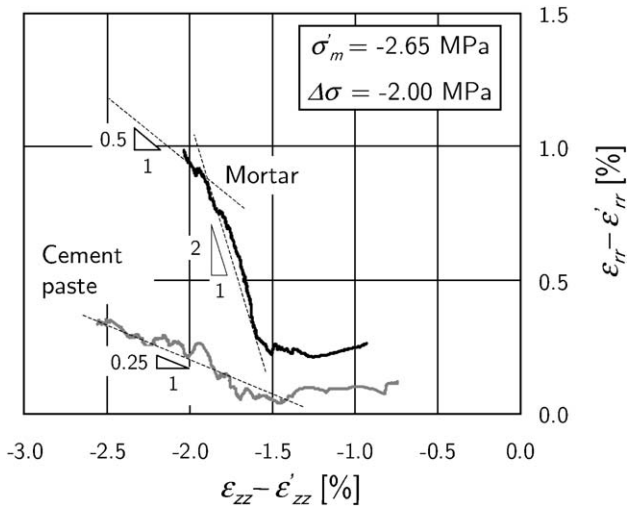

Fig. 8. Radial creep strain versus axial creep strain of cement paste and mortar.

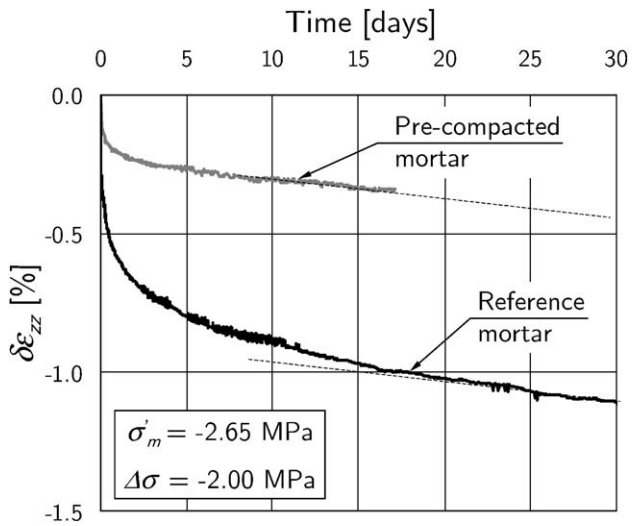

Fig. 9. Effect of precompaction of mortar on the change of axial strain during deviator creep tests.

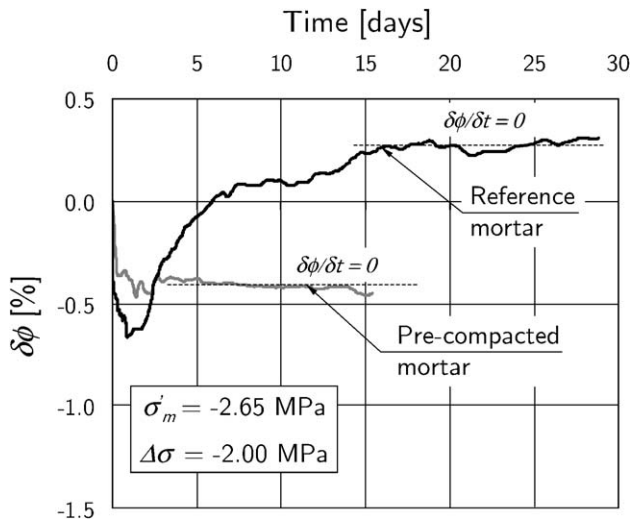

Fig. 10. Effect of precompaction of mortar on the porosity change during deviator creep tests.

3.3.1. Creep of precompacted mortar

Mortar that has been precompacted by high hydrostatic pressure does not exhibit a short-term dilating behavior. The long-term creep is not affected by precompaction.

Heukamp et al. [14] showed that a hydrostatic compression of $\sigma'_m = -9.0$ MPa makes the ITZ vanish due to pore collapse and the compaction of the surrounding cement paste matrix. In our study, mortar is hydrostatically preloaded to a mean stress of $\sigma'_m = -9.0$ MPa, then unloaded to the confinement level of $\bar{\sigma}_{rr} = -1.98$ MPa, at which the deviator stress $\Delta\sigma = -2.0$ MPa is applied and kept constant in time. Prior to deviator loading, the difference in initial porosity between the precompacted mortar specimen and the reference mortar is roughly 4.4%.

Figs. 9 and 10 compare the axial creep strain response $\delta\varepsilon_{zz}(t)$ and the porosity change $\delta\phi(t)$ of the precompacted mortar with the reference mortar sample:

1. While precompaction significantly reduces the very early axial creep strain magnitude, the long-term evolution of $\delta\varepsilon_{zz}(t)$ seems to be independent of the densification of the ITZ. Indeed, the precompacted sample follows a similar long-term creep kinetics $\delta\varepsilon_{zz}/\delta t$ as the reference sample (see Fig. 9).
2. In contrast to the reference sample, the precompacted mortar does not exhibit a short-term dilating behavior. The initial volume contraction ($\delta\phi/\delta t < 0$) stabilizes quickly, and the material creeps at constant volume early on (see Fig. 10).

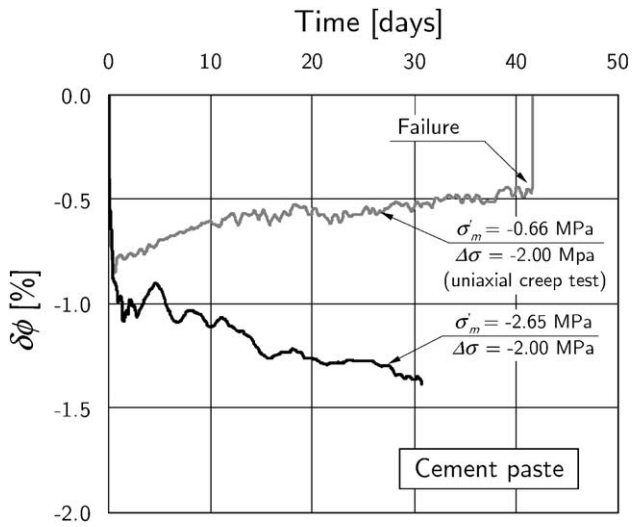

Fig. 11. Influence of confinement level on the porosity change $\delta\phi$ of cement paste.

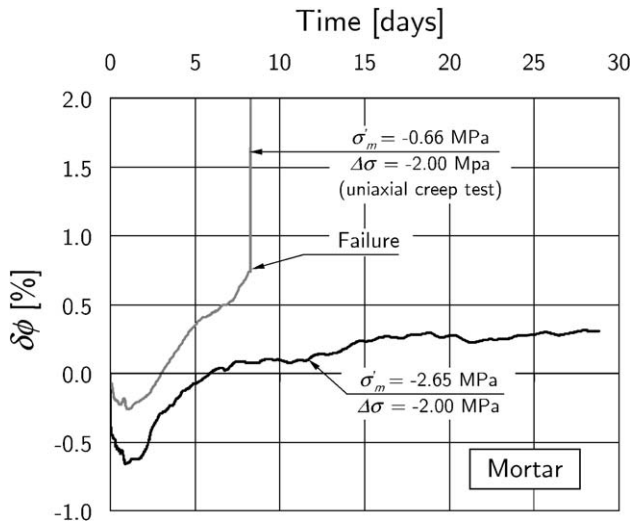

Fig. 12. Influence of confinement level on the porosity change $\delta\phi$ of mortar.

The results confirm that short-term dilation creep is highly influenced by the strength and the stiffness of the ITZ. By contrast, given the same long-term creep kinetics of both precompacted and reference sample, the physical mechanism at the origin of creep seems not to be situated in the ITZ but in the cement paste matrix.

3.3.2. Creep in low confinement triaxial tests

At low confinement, both cement paste and mortar exhibit an overall dilating behavior, and this behavior leads to creep failure in both materials.

Uniaxial compressive creep tests were performed at the same deviator stress level as before ($\Delta\sigma = -2.0$ MPa) but at a lower confinement level of $\sigma'_m = (1/3)\delta\sigma = -0.66$ MPa. This corresponds to a deviator stress-to-strength ratio of $n = 78\%$ for the cement paste, and $n = 77\%$ for the mortar.

Figs. 11 and 12 show the influence of the low confinement on the porosity change $\delta\phi(t)$ of the cement paste and the mortar:

1. Leached cement paste exhibits at low confinement ($\sigma'_m = -0.66$ MPa) a dilating behavior, in contrast to the contracting behavior found at higher confinement levels ($\sigma'_m = -2.65$ MPa in Fig. 11). This result is consistent with the deviator stress-induced dilatation shown in Fig. 5, but it reflects in the first place the higher shear stress component and deviator stress-to-strength ratio in the uniaxial compression test ($n = 78\%$ versus $n = 45\%$).
2. Figs. 11 and 12 show that the short-term dilating behavior of cement paste and mortar, at low confinement, can lead to creep failure that can clearly be attributed to the high shear stress.
3. Fig. 13 displays the radial strain versus the axial strain in the uniaxial tests. The slope in Fig. 13 is $\delta\varepsilon_{rr}(t)/\delta\varepsilon_{zz}(t) \simeq -0.85$ at short term and $\simeq -0.55$ later for the cement paste, and $\delta\varepsilon_{rr}(t)/\delta\varepsilon_{zz}(t) \simeq -2.0$ for the mortar. Given that the slope, for mortar, is the same in uniaxial compression and in deviator compression (see Fig. 8), the value appears to be independent of the confinement level, and just related to a characteristic dilating behavior of mortar induced by deviator load application. On the other hand, the value for the cement paste is much higher for low confinement than for high confinement. Finally, it could be tempting to associate these slopes with a CPR. However, the high values are nonadmissible, and highlight that standard isotropic viscoelasticity is inappropriate to capture the stress-induced anisotropic creep behavior of cement-based materials, which involves creep dilatation and deviator creep.

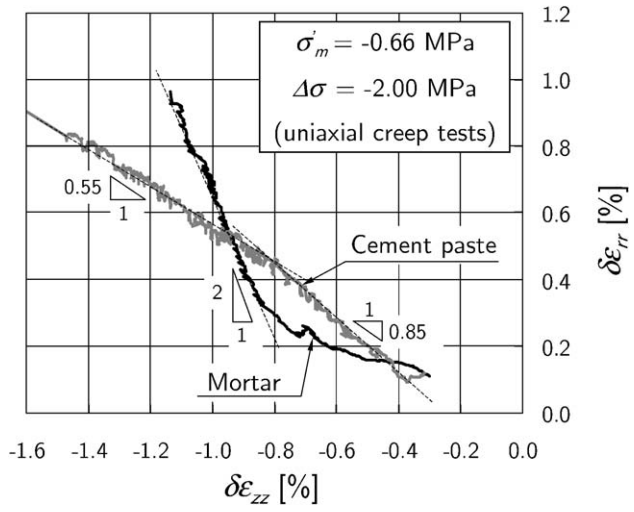

Fig. 13. Radial creep strain versus axial creep strain for cement paste and mortar (uniaxial creep tests).

4. Discussion

The results provide clear evidence of a specific short-term creep and a specific long-term creep that have different patterns and origins.

4.1. Short-term creep

The two elements that characterize the short-term creep of calcium-leached cement-based materials are (1) the contracting or dilating behavior that depends on the stress state and the heterogeneous microstructure of the material, and (2) the finite duration of roughly 3 weeks.

The highly porous cement paste is composed of a solid phase (i.e., the C–S–H) and a wide range of saturated pores (i.e., the intrinsic nanoporosity of C–S–H, the capillary pores, and the remaining pores left from the dissolution of Portlandite crystals). The mortar is composed of a cement paste matrix and sand inclusions. In a micromechanical sense, calcium-leached cement paste and mortar can be seen as two limit cases of a matrix inclusion composite morphology [17]: the large pores left from the dissolution of Portlandite of the cement paste represent (almost) infinitely soft inclusions in a C–S–H matrix, and sand particles in mortar represent (almost) infinitely rigid inclusions in a cement–paste matrix, separated by the ITZ. From micromechanics theory [18], it is well known that such a morphology leads to a nonuniform stress concentration in the microstructure that is locally much higher than the macroscopic stress application. It is suggested that this nonuniform microscopic stress distribution is the driving force of two different short-term relaxation mechanisms, creep and microcracking. This is elaborated on as follows.

- A purely hydrostatic initial state of compressive stresses induces at a microscopic level both volumetric stresses and deviator stresses [19]. It is suggested that the creep of C–S–H is a purely deviator phenomenon: it occurs at constant volume. The microdeviator stresses at loading triggers a relaxation by deviator creep of the nonuniform microstresses towards a state of uniform hydrostatic compression at the microscale. Once this hydrostatic microstress

state has been established, the time-dependent behavior stops. This microscopic creep relaxation process can explain the finite duration of 3 weeks of the short-term creep. The same time scale of this short-term creep mechanism for both cement paste and mortar provides strong evidence that the C–S–H is the only component of cement-based materials that exhibits creep [11]. Furthermore, the assumption of a pure deviator creep of the C–S–H means that the C–S–H matrix subjected to creep-provoking microscopic deviator loading expands into the micropores, in order to preserve its solid volume. It is this expansion into the micropores which is recorded in the hydrostatic creep test as a change of the Lagrangian porosity $\delta\phi < 0$ (i.e., the overall contracting behavior of the cement paste). In mortar, subjected to hydrostatic loading, the cement paste matrix can expand in the additional pore space of the ITZ, which is the weakest and the more porous zone in mortar [16]. This may explain the higher contraction of mortar during the first 10 days (see Fig. 3). In addition, the densification of the ITZ allows for a stress redistribution from the rigid inclusions to the softer cement paste matrix over the common interface, the ITZ.

- A macroscopic deviator stress, in addition to the hydrostatic compression, increases the microscopic creep-provoking stress deviator, and to a level where the relaxation of stresses, by creep, in the C–S–H is too slow to be supported by the material. This process activates a second stress relaxation mechanism in the microstructure—one associated with microcracking, which is macroscopically expressed by a dilating behavior $\delta\phi > 0$. The two relaxation mechanisms occur at different scales: the creep relaxation at the scale of the C–S–H matrix, the microcracking at the scale of the cement paste, and the interfaces with rigid inclusions in mortar. Particularly, in mortar, microcracks emerge predominantly from the ITZ, as SEM images show (see Fig. 14). At the same (high) macroscopic confinement, this explains the dominating dilating behavior of mortar compared to the contracting behavior of cement paste (see Fig. 3). Finally, this stress relaxation by microcracking is consistent with the aforementioned acoustic emission results of Rossi and Acker [10] and Denarié [20]. The former found a correlation over a 2-week measurement period between the succession of cracking events and the evolution of axial creep strains under load-imposed conditions (creep test). The latter found the same under displacement-imposed conditions (relaxation test).

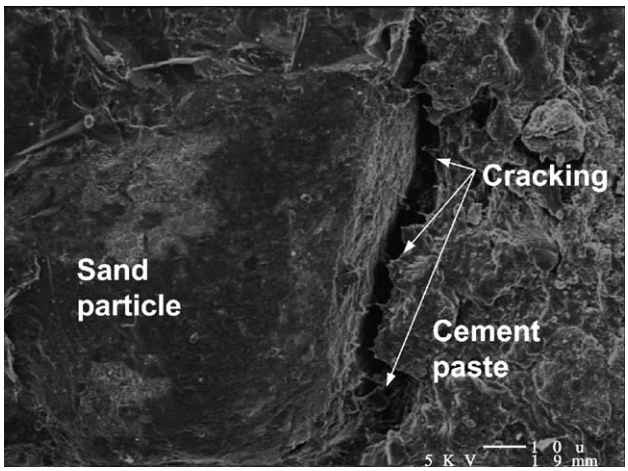

Fig. 14. Stabilized deviator-induced microcracking in the ITZ of mortar ($\sigma'_m = -2.65$ MPa, $\Delta\sigma = -2.0$ MPa).

- The two stress relaxation mechanisms (creep versus cracking) are in competition over time. The time-dependent failure identified for cement paste and mortar in low confinement triaxial creep tests (see Figs. 11 and 12) provides conclusive evidence of this competition involved in the short-term microcracking-related stress relaxation. Indeed, it appears that the microcracks, at low confinement, coalesce to form slippage planes along which the material fails in time. By contrast, a higher level of confinement prevents the faster crack propagation, and thus creep failure, by stabilizing the volume deformation due to microcracking. The switch from a contracting behavior to a dilating behavior that depends on the confinement level indicates the existence of a threshold in cement paste and mortar, beyond which microcracking dominates over volume contraction.

4.2. Long-term creep

The long-term creep of calcium-leached materials is characterized by a purely deviator creep that occurs at constant macroscopic volume for cement paste and mortar. The long-term creep of cement-based materials, therefore, appears to be governed by the deviator creep of the solid part of the cement paste (i.e., the C–S–H). This explains why both precompacted and reference mortar have the same long-term creep kinetics (see Fig. 9). These observations confirm earlier suggestions that the physical mechanism at the origin of long-term creep was situated in the C–S–H solid phase [11], which is not affected by precompaction, in contrast to the ITZ. The results are consistent with the creep mechanism proposed by Bažant et al. [2]: the long-term deviator creep originates in the C–S–H solid phase of the cement paste from sliding of the C–S–H sheets driven by local shear stresses. The sliding is the result of atomic bond breakage and bond reformation in between close parallel surfaces of C–S–H. As this process relaxes locally the average bond force, another creep site becomes overstressed due to stress redistribution, causing again a bond to break. While this creep mechanism can a priori accommodate both volume and deviator creep, our experimental results suggest that only deviator long-term creep occurs in cement-based materials.

5. Conclusion

The presented results were obtained on calcium-leached materials, but the results are all consistent with both experimental results [8,10] and theoretical investigations [2] on concrete. This confirms that the relevant deformation

characteristics of creep of nondegraded cement-based materials are preserved in calcium-leached materials.

The triaxial creep results provide strong experimental evidence that at least two competing dissipative mechanisms are at work in short-term creep of cement-based materials: (1) a creep relaxation mechanism in the C–S–H solid phase related to microstress concentrations in the heterogeneous microstructure; and (2) stress relaxation by microcracking beyond a relatively small stress threshold. From a theoretical point of view, these results reconcile two schools of thinking, which assumed that only one of the two proposed dissipative mechanism was at work. From a practical point of view, it appears that microcracking is involved in creep of most concrete structures, which are usually not subjected to purely volumetric stress states. Indeed, our experimental results suggest that microcracking is involved in the short-term creep of mortar for a deviator stress-to-strength ratio of $n = 37\%$, which is quite similar to the deviator stress-to-strength ratio characterizing the service state of concrete structures. The good news is, however, that this microcracking is primarily involved in short-term creep. Provided that microcracks stabilize during the finite duration of some 3 weeks, creep occurs thereafter at constant volume. Both short-term contracting-dilating creep and long-term constant volume creep cannot be captured by a CPR—and this concept, therefore, should be abandoned when triaxial stress states affect the durability performance of concrete structures.

Acknowledgements

Financial support for this study was provided through a Postdoctoral Fellowship for Dr. Olivier Bernard of the Swiss National Science Foundation (SNF), mediated through the research committee of the Swiss Federal Institute of Technology in Lausanne, and by the Nuclear Energy Research Initiative Program of the US Department of Energy (DOE). The authors also gratefully acknowledge Dr. F.H. Heukamp, former graduate student in the Department of Civil and Environmental Engineering at MIT, for helpful comments and suggestions in the performance of the triaxial creep tests.

References

[1] P. Acker, F.-J. Ulm, Creep and shrinkage of concrete: Physical origins, practical measurements, Nucl. Eng. Des. 203 (2–3) (2001) 143–158.
[2] Z.P. Bažant, A.B. Hauggaard, S. Baweja, F.-J. Ulm, Microprestress-solidification theory for concrete creep: I. Aging and drying effects, J. Eng. Mech., ASCE 123 (11) (1997) 1188–1194.
[3] L. Granger, Time-dependent behavior of concrete in nuclear tanks: Analysis and modeling, Research Report LPC OA21, Laboratoire Central des Ponts et Chaussées, Paris, 1996 (in French).
[4] O. Bernard, E. Brühwiler, The effect of reinforcement in the new layer on hygral cracking in hybrid structural elements, Mater. Struct. 36 (256) (2003) (in press).
[5] A.M. Neville, W.H. Dilger, J.J. Brooks, Creep of Plain and Structural Concrete, Construction Press, London, 1983.
[6] K.S. Gopalakrishnan, A.M. Neville, A. Ghali, Creep Poisson's ratio of concrete under multiaxial compression, ACI J., (66) (1969) 1008–1020.
[7] J.W. Chuang, T.W. Kennedy, E.S. Perry, J.N. Thomson, Prediction of multiaxial creep from uniaxial creep tests. Concrete for nuclear reactors, Am. Concr. Inst. Publ. SP-34, (1972) 701–734.
[8] F.-J. Ulm, F. Le Maou, C. Boulay, Creep and shrinkage couplings: New review of some evidence, Rev. Fr. Genie Civ. 3 (3–4) (1999) 21–37.
[9] F.-J. Ulm, F. Le Maou, C. Boulay, Creep and shrinkage of concrete—kinetics approach, Creep and Shrinkage—Structural Design Effects, Proceedings of the Adam Neville Symposium, ACI-SP-194, 2000, pp. 135–153.
[10] P. Rossi, P. Acker, A new approach to the basic creep and relaxation of concrete, Cem. Concr. Res. 18 (5) (1988) 799–803.
[11] P. Acker, Micromechanical analysis of creep and shrinkage mechanisms, in: F.-J. Ulm, Z.P. Bažant, F.H. Wittmann (Eds.), Creep, Shrinkage and Durability Mechanics of Concrete and Other Quasi-Brittle Materials, Proceedings of the Sixth International Conference CONCREEP6, Elsevier, 2001, pp. 15–25.
[12] F.-J. Ulm, F.H. Heukamp, J.T. Germaine, Residual design strength of cement-based materials for nuclear waste storage systems, Nucl. Eng. Des. 211 (1) (2002) 51–60.
[13] F.H. Heukamp, F.-J. Ulm, J.T. Germaine, Mechanical properties of calcium-leached cement pastes: Triaxial stress states and the influence of the pore pressure, Cem. Concr. Res. 31 (5) (2001) 767–775.
[14] F.H. Heukamp, F.-J. Ulm, J.T. Germaine, Poroplastic properties of calcium-leached cement-based materials, Cem. Concr. Res. (2003) (in press).
[15] O. Coussy, Mechanics of Porous Media, Wiley, Chichester, UK, 1995.
[16] J. Maso (Ed.), Interfacial transition zone in concrete, State of the Art Report of the RILEM Technical Committee 108-ICC, Interfaces in Cementitious Composites, E&FN Spon, London, 1996.
[17] G. Constantinides, F.-J. Ulm, The effect of two types of C–S–H on the elasticity of cement-based materials: Results from nanoindentation and micromechanical modeling, Cem. Concr. Res. (2002) (submitted for publication).
[18] P. Suquet (Ed.), Continuum Micromechanics, Springer-Verlag, Wien, 1997.
[19] E. Lemarchand, F.-J. Ulm, L. Dormieux, The effect of inclusions on the friction coefficient of highly filled composite materials, J. Eng. Mech., ASCE 128 (8) (2002) 876–884.
[20] E. Denarié, Experimental study of couplings between viscoelasticity and crack growth in concrete, PhD Thesis, Swiss Federal Institute of Technology, Lausanne, 2000 (in French).